RSC Advances

ROYAL SOCIETY OF CHEMISTRY

www.rsc.org/advances

Graphical Abstract

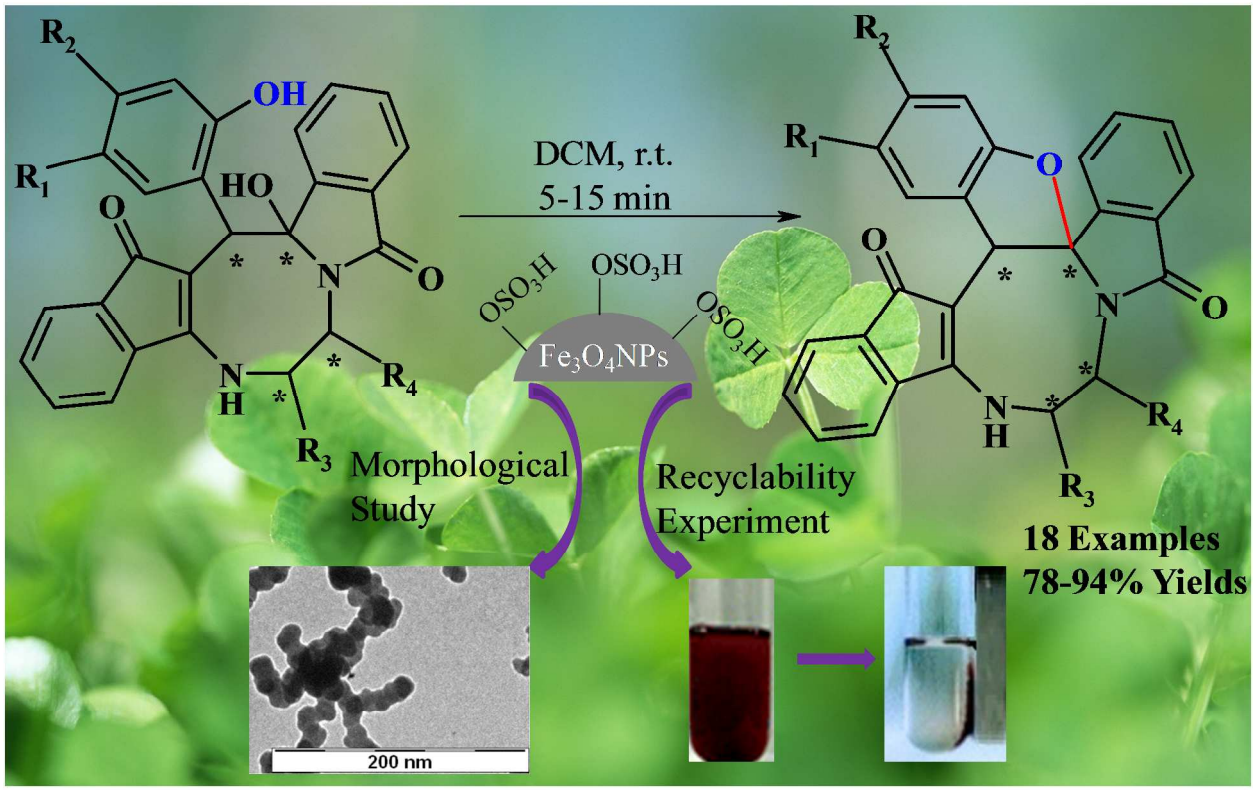

Facile cyclization in the synthesis of highly fused diaza cyclooctanoid compounds using retrievable nano magnetite-supported sulfonic acid catalyst

Sudipta Pathak,[a] Kamalesh Debnath,[a] Md. Masud Rahaman Mollick[b] and Animesh Pramanik* [a]

[a]*Department of Chemistry and* [b]*Department of Polymer Science & Technology, University of Calcutta, 92, A. P. C. Road, Kolkata-700 009, India;* Fax: +91-33-2351-9755; Tel: +91-33-2484-1647.

E-mail: animesh_in2001@yahoo.co.in

Abstract: Magnetically separable Fe_3O_4-SO_3H nano particles has been prepared and established as an efficient catalyst for the synthesis of dihydrofuran fused cyclooctanoids via dehydration reaction of dihydroxy cyclooctanoid heterocylces. Nanomagnetite, Fe_3O_4-SO_3H was prepared using an impregnation protocol and fully characterized by XRD, FT-IR, TEM, and FE-SEM-EDS. The catalyst was recycled for five consecutive cycles with almost unaltered catalytic activity. The dehydration step was performed keeping the acid sensitive amide linkage intact under ambient temperature and milder reaction condition. The efficacy of the methodology lies in excellent yield of product formation within short span of reaction time avoiding undesirable side products due to the substrate decomposition by ring rupture and tedious purification and work-up procedure.

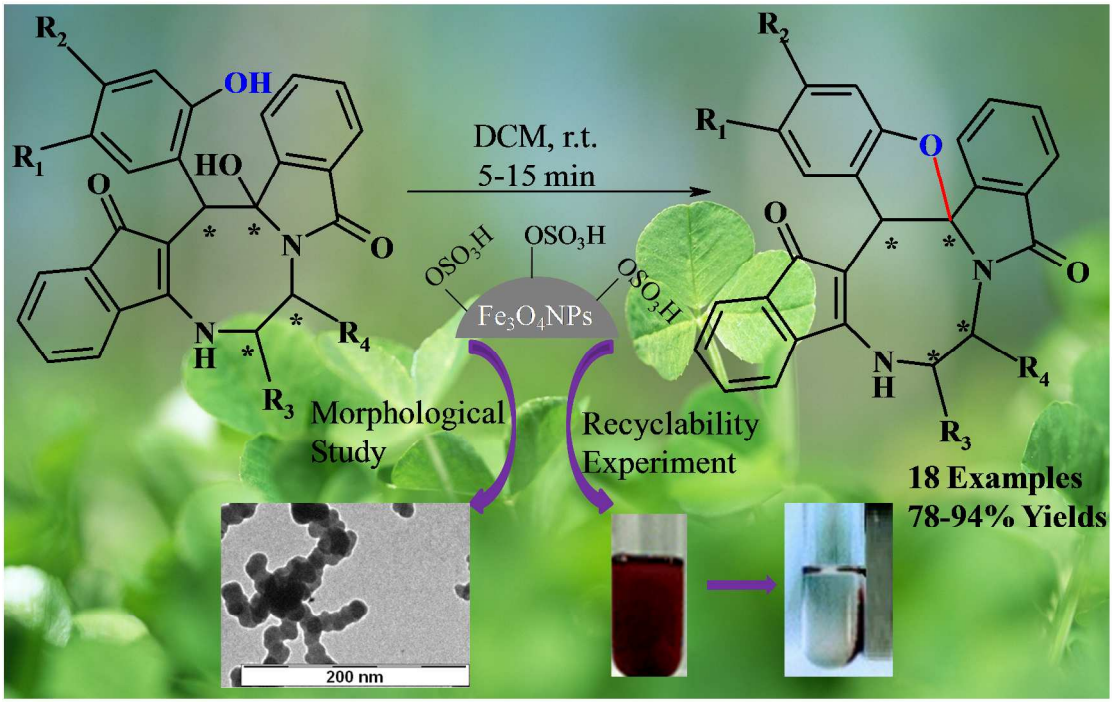

Introduction

The functionalized cyclooctanes are frequently found in pharmacologically significant compounds and natural products. Because of their intriguing geometrical features and potential biological activities, the construction of cyclooctanoid framework has drawn significant attention of the synthetic organic chemists for a long time.[1,2] In many natural products eight-membered carbo and heterocycles are fused with one or more five- or six-membered rings. For examples, the cyclooctanoid fusicoauritone (**1**),[3] aleurodiscal (**2**),[4] *Kopsia* alkaloid specially lapidilectam (**3**),[5] ophiobolin A (**4**),[6] serotobenine (**5**)[7] and deoxyisoaustamide (**6**)[8] are natural compounds containing fused penta- and hexacyclic rings (Fig. 1). Extensive investigation on the above mentioned eight membered hetero or carbocycle family shows that they have broad spectrum of bioactivity against fungi, nematodes, bacteria, the *Plasmodium falciparum* and cultutred B-16 melanoma cells.[6,9,10] Marine-products cyclooctanoid (**6**) containing indole ring are presently considered as the affluent sources of active secondary metabolites (Fig. 1).[8] Therefore, synthesis

of cyclooctanoids fused with penta- and hexacyclic ring is very important. In recent years a variety of synthetic methodologies have been developed for the synthesis of fused cyclooctanoid rings which include olefin metathesis,[11] cycloadditions,[12] nucleophilic and electrophilic substitution reactions,[13] a Mizoroki-Heck reaction,[14] ring expansion reactions[15] and other reactions.[16] In our continuing endeavor to synthesize biologically potent heterocyclic compounds from ninhydrin,[17] we wish to report herein a cyclization method for the synthesis of isoindole and benzofuran fused eight-membered spiro heterocycles following the Green Chemistry principles.

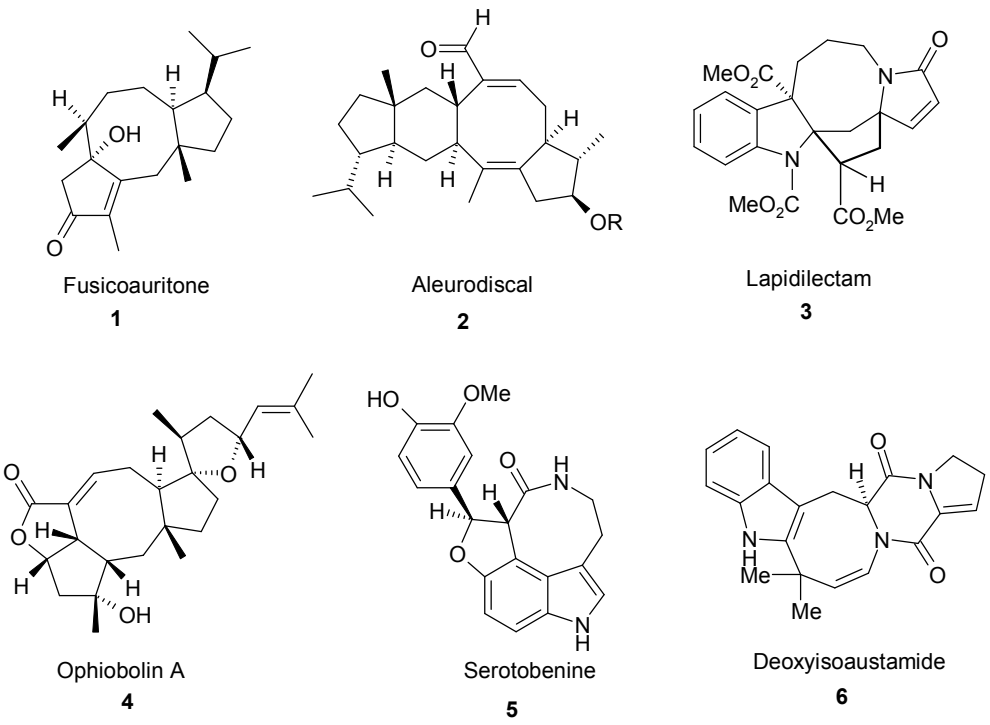

Fig. 1 Some important naturally occurring eight-membered heterocycles.

Catalysis is becoming a strategic field of science because it represents a new way to meet the challenges of energy and sustainability. In order to explore environmentally benign synthetic pathways, we need a catalyst system that not only shows high activity and selectivity (like a

homogeneous system) but also can be separated and recovered easily after the reactions (like a heterogeneous system). In this respect nanocatalysts have recently been emerged as highly promising catalysts which mimic both homogeneous (high surface area, easily accessible) and heterogeneous (stable, easy to handle) catalyst systems. The main difficulty in the nanocatalyst mediated organic reaction is the separation and recovery of the catalyst through conventional filtration as it blocks the pores and valves of the filter papers. In this respect, the use of magnetically separable nanoparticles (MSNPs) such as iron oxide supported nano materials attributes excellent isolation and separation procedure from the reaction mixture by means of an external magnet because of their insolubility and paramagnetic nature. Moreover, they are inexpensive, easy to prepare, and most importantly easily recyclable for many times.[18]

Chlorosulfonic acid is a well-known strong organic acid, which is used as an active catalyst in organic syntheses. However, its direct application in the reaction mixture may cause the decomposition of the reactants and also derivation of several impurities. The best way to avoid the harmful effect of chlorosulfonic acid is by supporting it on a solid surface.[19] In this regard, magnetically retrievable Fe_3O_4@SO_3H emerges as an efficient and sustainable acid catalyst for many organic reactions.[19,20] Here, we have exploited this acid catalyst for the construction of dihydrofuran ring in cyclooctanoid compounds (±)-**2a-r**/**2a′-r′** starting from dihydroxy cyclooctanoid heterocylces (±)-**1a-r**/**1a′-r′** (Scheme 1).

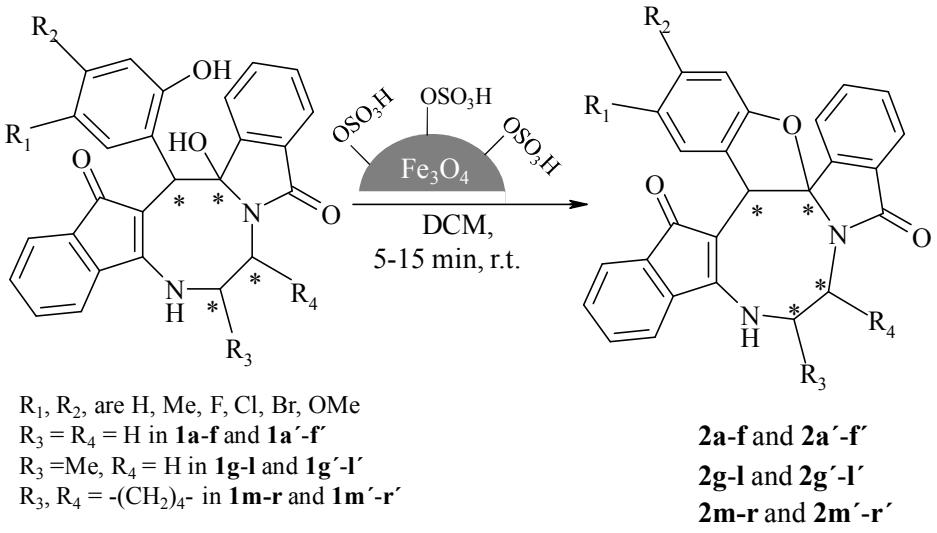

R_1, R_2, are H, Me, F, Cl, Br, OMe
$R_3 = R_4 = H$ in **1a-f** and **1a´-f´**
R_3 =Me, R_4 = H in **1g-l** and **1g´-l´**
R_3, R_4 = -$(CH_2)_4$- in **1m-r** and **1m´-r´**

2a-f and **2a´-f´**
2g-l and **2g´-l´**
2m-r and **2m´-r´**

Scheme 1 Optimized reaction condition for the formation of fused cyclooctanoids.

Results and discussion

In our initial study, we attempted to optimize the reaction conditions for the formation of (±)-**2a**/**2a′** (R_1=Me, R_2=R_3=R_4=H) from (±)-**1a**/**1a′** (R_1=Me, R_2=R_3=R_4=H) in presence of different solvents, catalysts, solid supports at different temperature and time (Scheme 1, Table 1). From literature survey, it is known that, to carry out dehydration reaction in Dean-Stark apparatus, benzene is the most commonly used solvent. So at first, we tried to carry out the dehydration in (±)-**1a**/**1a′** using benzene as the solvent. Unfortunately, no product was isolated after prolonged reflux (Table 1, entry 1). Then we tried to carry out the dehydration and subsequent intra-molecular etheration reaction under acid catalyzed condition in presence of several organo-acid catalysts such as lactic acid, formic acid, citric acid and acetic acid in benzene (Table 1, entries 2-5). In all the cases, trace amount of desired product was isolated through column chromatography and the structure of the product **2a** and **2a′** was confirmed by IR, ^{1}H and ^{13}C NMR spectroscopy, elemental analysis, and X-ray diffraction studies. To obtain

the desired product with satisfactory yield, we employed higher acidic condition in the reaction, using acetic acid as solvent (Table 1, entry 6). But yield of the product (±)-**2a**/**2a′** was still very low (30%) and unsatisfactory. When stronger Brønsted acid catalyst PTSA was used in benzene, moderate yield (48 %) of the desired product was obtained (Table 1, entry 7), which increased further (65-68%) in dichloromethane (DCM) and dimethylformamide (DMF) solvent because of better solubility of the starting material (Table 1, entries 8 and 9). Since the yields are comparable in these two solvents, DCM was chosen as the best solvent for our reaction because of operational simplicity and easier work-up procedure. It was also clear from these studies that, -SO_3H functional group is acting as a better activating agent compared to –COOH group. So next, we employed several solid supports bearing –SO_3H group such as homogeneous polymeric acid-surfactant combined catalyst PEG-SO_3H and heterogeneous solid acid supports MSA and SSA as catalyst in DCM (Table 1, entries 11-13). Moderate yield of the product (±)-**2a**/**2a′** under reduced reaction time and temperature in presence of SSA (Table 1, entry 13) incited us for further investigation on the optimization of the reaction condition using magnetic nano-catalysts bearing –SO_3H group on the surface. In this regard, two nano-catalysts Fe_3O_4-SO_3H and γ-Fe_3O_4@SiO_2-SO_3H[21,22] were considered since they have interesting structural features, high level of catalytic activity for large surface area and facile separation procedure using external magnets (Table 1, entries 14-20). Gratifyingly, significant increase in the product yield (92%) was obtained with drastic diminution of required temperature (30 °C) and reaction time (10 min) on employing nano-magnetite Fe_3O_4-SO_3H (50 mg) in DCM (Table 1, entry 18) after careful tuning of catalyst load (20-150 mg) under same reaction condition (Table 1, entries 14-19). Interestingly, comparable yield of (±)-**2a**/**2a′** was observed using magnetically retrievable γ-Fe_3O_4@SiO_2-SO_3H as catalyst (Table 1, entry 20). Since nano-magnetite Fe_3O_4-SO_3H is easier

to prepare compared to γ-Fe_3O_4@SiO_2-SO_3H, the former was chosen as the most suitable catalyst for the present reaction.

Table 1 Optimization studies for etheration reaction in (±)-**1a**/**1a′** to form (±)-**2a**/**2a′**

Entry	Catalyst	Solvent	Catalyst load	Temperature (ºC)	Time	Yield (%)[a]
1	—	Benzene	—	80	24 h	—
2	Lactic acid	Benzene	20 mol %	80	24 h	10
3	Formic acid	Benzene	20 mol %	80	24 h	8
4	Citric acid	Benzene	20 mol %	80	24 h	10
5	Acetic acid	Benzene	20 mol %	80	24 h	10
6	—	Acetic acid	—	80	24 h	30
7	PTSA	Benzene	20 mol %	80	24 h	48
8	PTSA	DCM	20 mol %	40	24 h	65
9	PTSA	DMF	20 mol %	80	24 h	68
10	PTSA	H_2O	20 mol %	80	24 h	45
11	PEG-SO_3H	DCM	500 mg	40	24 h	35
12	Melamine sulphonic acid (MSA)	DCM	500 mg	40	24 h	27
13	Silica sulfuric acid (SSA)	DCM	500 mg	40	3 h	47
14	Fe_3O_4-SO_3H	DCM	100 mg	40	10 min	72
15	Fe_3O_4-SO_3H	DCM	100 mg	30	10 min	72
16	Fe_3O_4-SO_3H	DCM	150 mg	30	10 min	71
17	Fe_3O_4-SO_3H	DCM	75 mg	30	10 min	80
18	**Fe_3O_4-SO_3H**	**DCM**	**50 mg**	**30**	**10 min**	**92**

19	Fe_3O_4-SO_3H	DCM	20 mg	30	10 min	85
20	γ-Fe_3O_4@SiO_2-SO_3H	DCM	50 mg	30	10 min	92

[a] Isolated yields

Having prepared (±)-**2a**/**2a′** successfully, we decided to explore the scope and generality of this reaction in the synthesis of other analogues. At first, racemic mixtures of diaza-cyclooctanoid derivatives (±)-**1a-r**/**1a′-r′** have been prepared from ninhydrin following the reported procedure.[17b] The diaza-cyclooctanoid compounds (±)-**1a-r**/**1a′-r′** derived from different aliphatic 1,2-diamines (1,2-ethylenediamine, (±)-1,2-propylenediamine and (±)-trans-1,2-cyclohexanediamine) were treated with Fe_3O_4-SO_3H under optimized reaction condition (Table 1, entry 18) to get fused eight membered heterocycles. As evident from Table 2, etheration reaction proceeded well with various electron-withdrawing and donating phenols and 1,2-diamine derivatives (Scheme 1, Table 2). In all the cases reaction time is short (10 min) and yield of the product formation is high (Table 2). The isolated yellow colored solid products (±)-**2a-r**/**2a′-r′** are fully characterized by ^{1}H and ^{13}C NMR spectroscopy. When diaza-cyclooctanoids (±)-(*R,S*)-**1a-f**/(*S,R*)-**1a′-f′** cyclized in presence of Fe_3O_4-SO_3H (±)-(*R,S*)-**2a-f**/(*S,R*)-**2a′-f′** were formed which is established by X-ray crystal data analysis (Fig. 2). The other possible diastereomer (*R,R* or *S,S*) is not formed in the reactions. Therefore, retention of configuration takes place at the chiral centre adjacent to amide nitrogen (Scheme 2). The same reaction was also carried out for (±)-(*R,S,S*)-**1g-l**/(*S,R,R*)-**1g′-l′**, as predicted from the above results reaction passed through retention of configuration to furnish (±)-(*R,S,S*)-**2g-l**/(*S,R,R*)-**2g′-l′** (Scheme 2, Fig. 3). Then etheration reaction was carried out with compounds having four stereo-centre (±)- (*R,S,S,S*)-**1m-r**/(*S,R,R,R*)-**1m′-r′**. As expected, products (±)-(*R,S,S,S*)-**2m-r**/(*S,R,R,R*)-**2m′-r′** were isolated from the

reaction mixture which is established by X-ray crystal structure analysis (Fig. 4). So it is clear from the above information that the cyclization reaction is enantioselective.

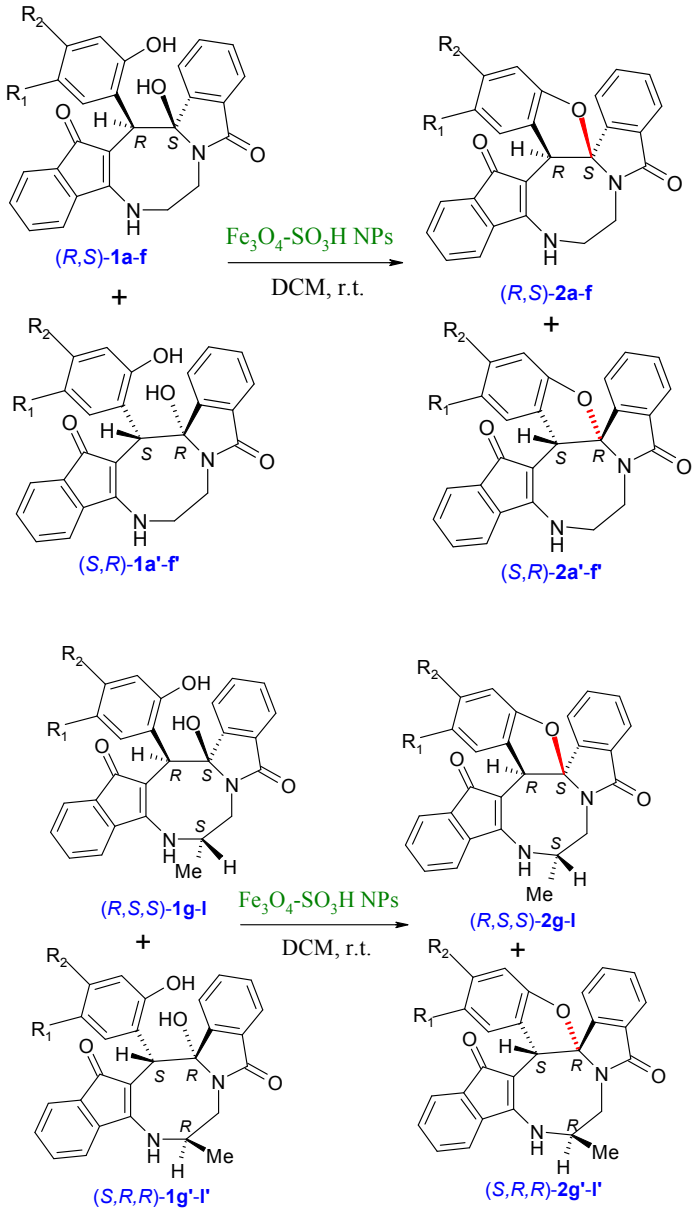

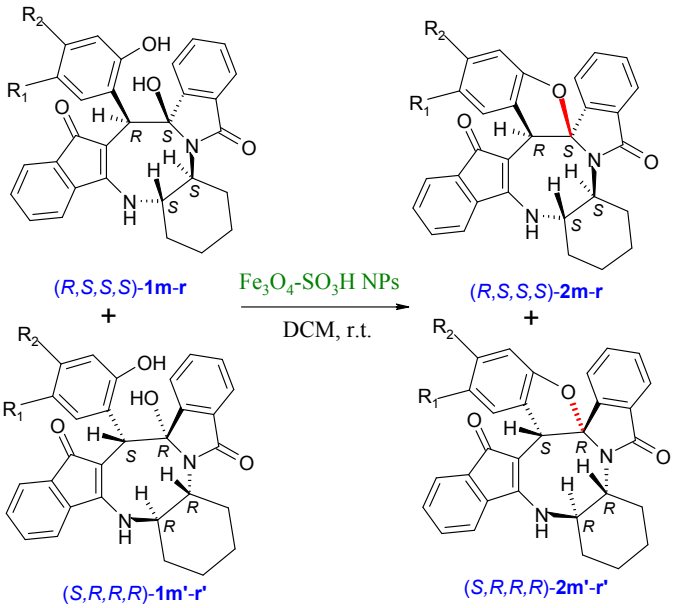

Scheme 2 Synthesis of isoindole fused cyclooctanoid rings as a racemic mixture.

Table 2 Scope of highly fused cyclooctanoid rings syntheses

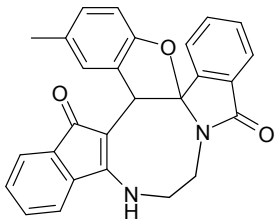
(±)-**2a**/**2a′** (92%)

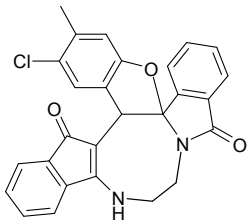
(±)-**2b**/**2b′** (90%)

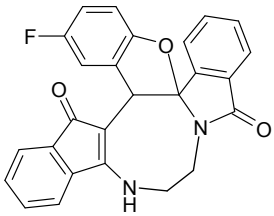
(±)-**2c**/**2c′** (89%)

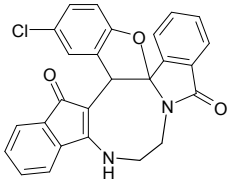
(±)-**2d**/**2d′** (91%)

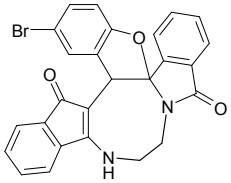
(±)-**2e**/**2e′** (92%)

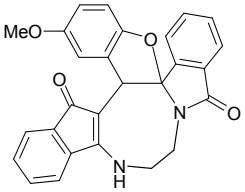
(±)-**2f**/**2f′** (94%)

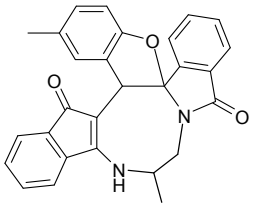
(±)-**2g**/**2g′** (89%)

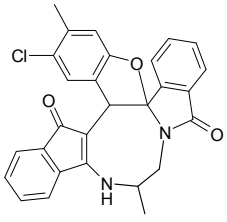
(±)-**2h**/**2h′** (86%)

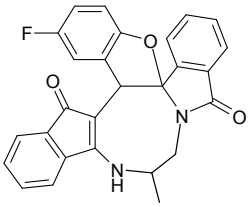
(±)-**2i**/**2i′** (84%)

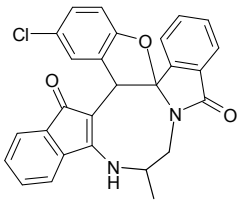

(±)-**2j/2j′** (85%)

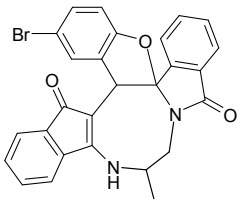

(±)-**2k/2k′** (88%)

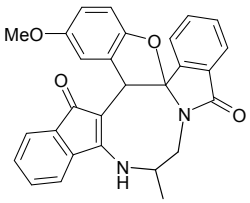

(±)-**2l/2l′** (92%)

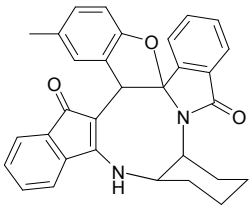

(±)-**2m/2m′** (85%)

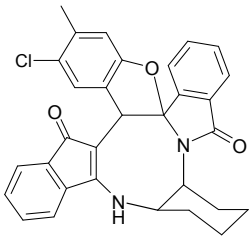

(±)-**2n/2n′** (81%)

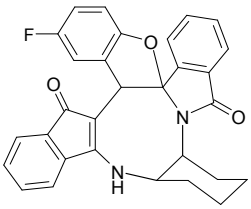

(±)-**2o/2o′** (78%)

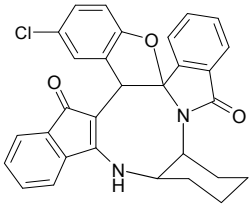

(±)-**2p/2p′** (80%)

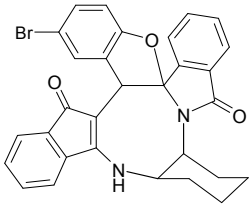

(±)-**2q/2q′** (83%)

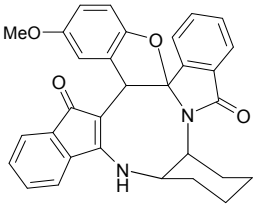

(±)-**2r/2r′** (89%)

A possible mechanism for the formation of spirofuran fused eight-membered heterocycles **2** from dihydroxy eight-membered heterocycles **1** is depicted in Scheme 3. The initially formed hydrogen bond between aliphatic hydroxyl and $–SO_3H$ group provokes the breaking of C-O bond to generate dehydrated cationic intermediate **3**. Finally, intramolecular nucleophilic attack of hydroxyl group of phenol to the imine carbon produces the oxonium intermediate **4** which subsequently loses proton to form furan ring fused eight-membered heterocycles **2**. During the intramolecular nucleophilic attack via S_N1 process, the phenolic hydroxyl group attacks from the same face of the double bond where the aromatic phenols are aligned, as a result retention of configuration takes place at the stereogenic centre.

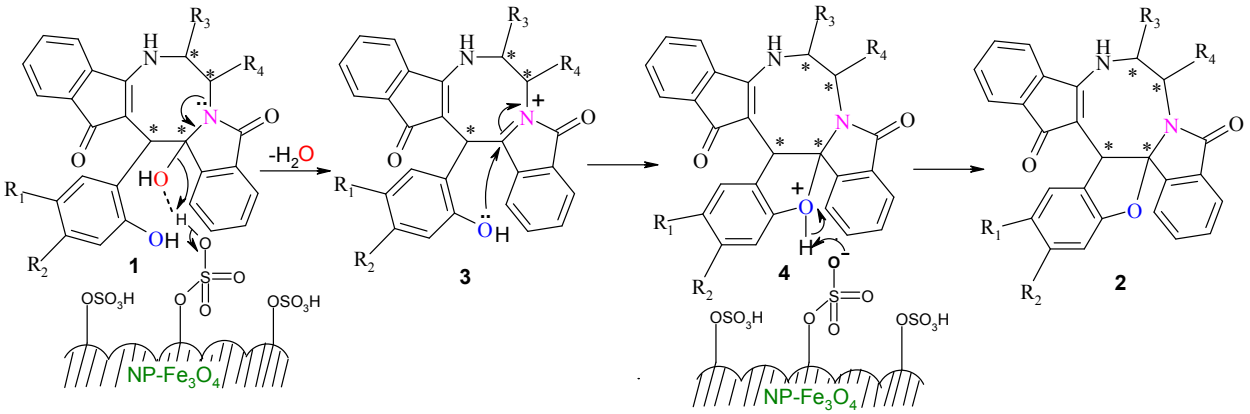

Scheme 3 Plausible mechanism for the formation of furan ring using NP Fe_3O_4-SO_3H as catalyst

The crystal structure analysis of (±)-**2a/2a′**, (±)-**2g/2g′** and (±)-**2n/2n′** reveals that in the crystalline state two enantiomeric molecules are locked in antiparallel fashion stabilized by two intermolecular hydrogen bonds between –NH– and C=O groups (Figs 2-4). The hydrogen bonding distance increases with the increase of the bulkiness of the substituents on 1,2-diamine moieties. In all the cases the central diazacyclooctane rings adopt a tub or boat like conformation rather than crown or boat-chair conformation (Figs. 2-4). The substituents around the diazacyclooctane rings are alternatively in up and down orientation due to steric reasons. In (*R*,*S*,*S*,*S*)-**2n** and (*S*,*R*,*R*,*R*)-**2n′** the central boat diazacyclooctane ring is further fused with chair cyclohexane ring (Fig. 4).

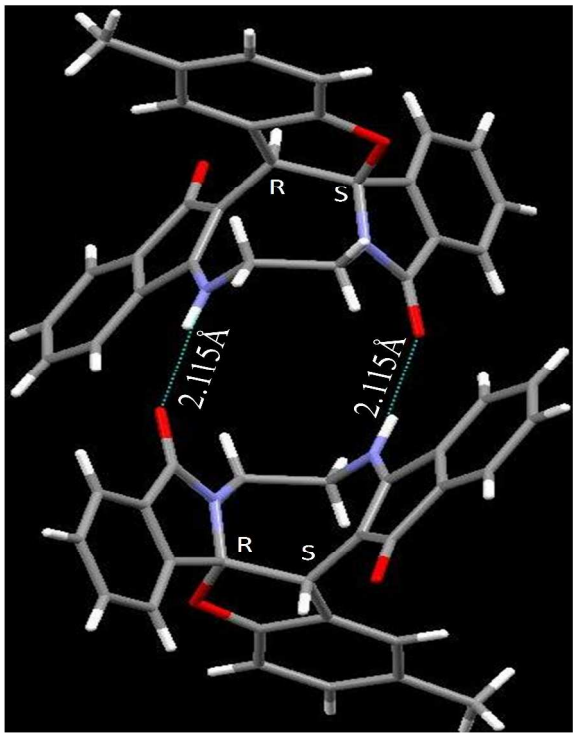

Fig. 2 Crystal structure of compound **2a** and **2a′**. Color code: red, oxygen; blue, nitrogen; grey, carbon; white, hydrogen (CCDC 994163).

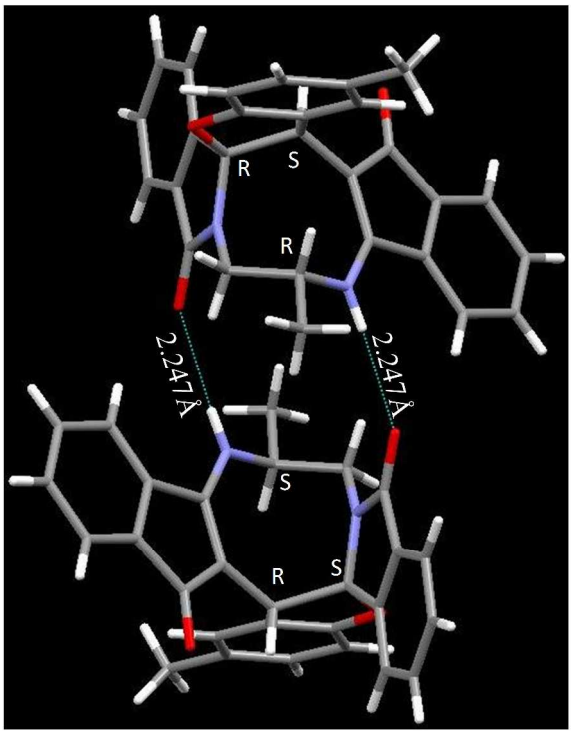

Fig. 3 Crystal structure of compound **2g** and **2g′**. Color code: red, oxygen; blue, nitrogen; green, chlorine; large white, carbon; small white, hydrogen (CCDC 994164).

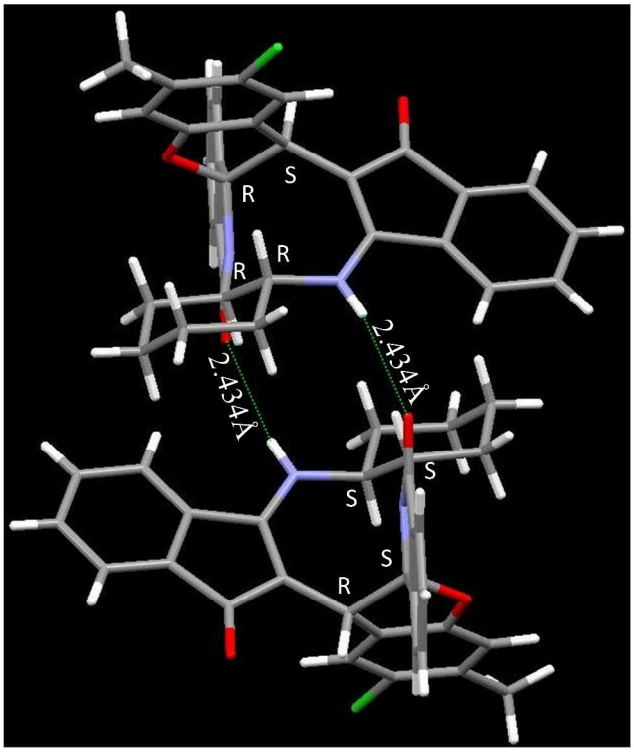

Fig. 4 Cystal structure of compound **2n** and **2n′**. Color code: red, oxygen; blue, nitrogen; green, chlorine; large white, carbon; small white, hydrogen (CCDC 994165).

The reusability test of Fe_3O_4-SO_3H nanoparticles was carried out under optimized conditions by stirring (±)-**1a**/**1a′** in DCM medium (Table 1, entry 18). When the magnetic stirring of the reaction mixture was discontinued, the magnetic Fe_3O_4-SO_3H MNPs were adsorbed on the surface of the magnetic stirring bar and separated easily from the reaction mixture without filtration. Then Fe_3O_4-SO_3H MNPs catalyst was washed three times with ethanol (3 X 5 mL), dried at room temperature under vacuum to eliminate residual solvents and used for the next

cycle. The dehydration reaction of (±)-**1a**/**1a′** was performed with recovered catalyst upto five times without any significant loss of the catalytic activity (**Fig. 5**).

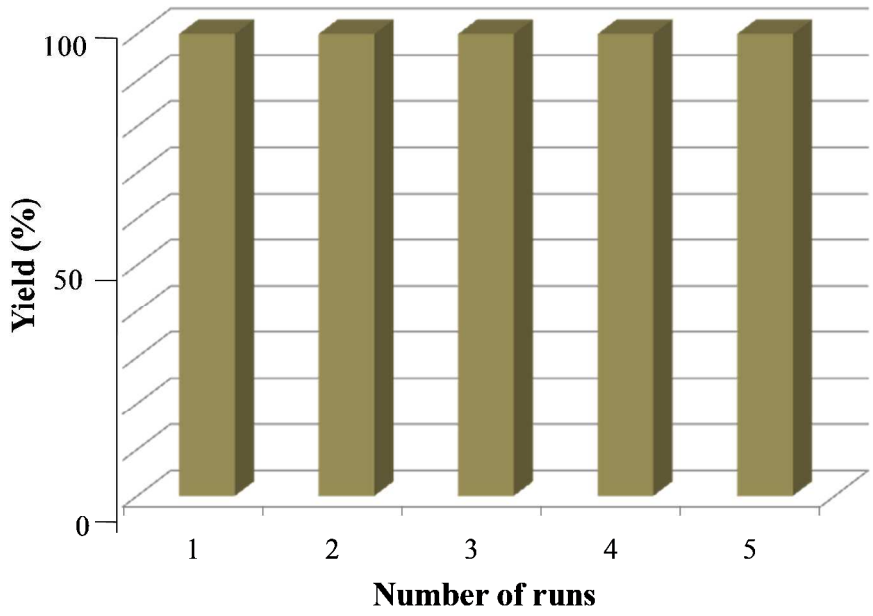

Fig. 5 Reusability of Fe_3O_4-SO_3H MNPs for the formation of densely fused cyclooctanoid.

Powder XRD study was carried out to confirm the crystalline nature of as-synthesized iron oxide nanoparticles. The XRD pattern of Fe_3O_4 and Fe_3O_4-SO_3H NPs are displayed in Fig. 6a and Fig. 6b respectively. The diffraction peaks from the (220), (311), (400), (422) and (440) lattice planes are observed at 2θ = 32.9°, 35.36°, 44.9°, 53.7° and 62.35° respectively (Fig. 6a). The peaks in the respective XRD patterns are equivalent to the Bragg reflections of face centered cubic (FCC) iron oxide and confirm both the identity and purity of the sample. Similar pattern of peaks is also obtained in Fe_3O_4-SO_3H NPs XRD spectra (Fig. 6b), with slight alterations in the nature of peaks. The presence of sulfonic acid group coated on the surface of Fe_3O_4 NPs might cause slight changes in the XRD spectra of Fe_3O_4-SO_3H NPs.[19]

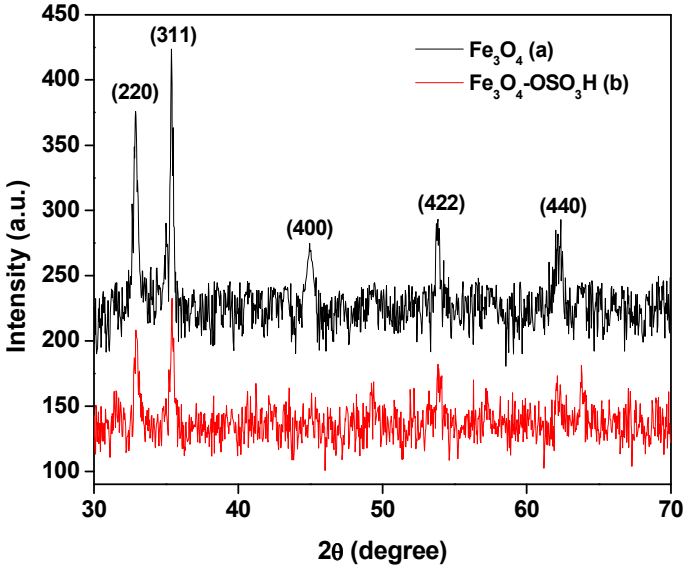

Fig. 6 XRD spectra of (a) Fe_3O_4 and (b) Nanocat- Fe_3O_4-SO_3H MNPs.

Field Emission Scanning electron microscopy (FE-SEM) at operating voltage of 5.0 kV is employed to know the morphology and size of Nanocat-Fe_3O_4-SO_3H nanoparticles (Fig. 7a). It is clear from the image in Fig. 7a that the spherical shaped Nanocat-Fe_3O_4-SO_3H nanoparticles have diameter in the range of ~23 to ~43 nm. Energy dispersive spectroscopy (EDS) analysis of the prepared Nanocat-Fe_3O_4-SO_3H nano-particle (sulfur peak) confirms the incorporation of -SO_3H group on the surface which comes from the reaction of Fe_3O_4 NPs with chlorosulfonic acid (Fig. 7b).

In order to confirm the formation of Nanocat-Fe_3O_4-SO_3H nanoparticles and to inspect its morphology, high-resolution transmission electron microscopic (HRTEM) analysis is performed (Fig. 7c and 7d). TEM analysis reveals that the prepared nanoparticles are uniform in size and mostly spherical in shape and the size of the nanoparticles is in the range of ~14 to ~23 nm. The characterization of the nano-Fe_3O_4-SO_3H by TEM images, before (Fig. 7c) and after five times applications **(**Fig. 7d) shows the unaltered particle size.

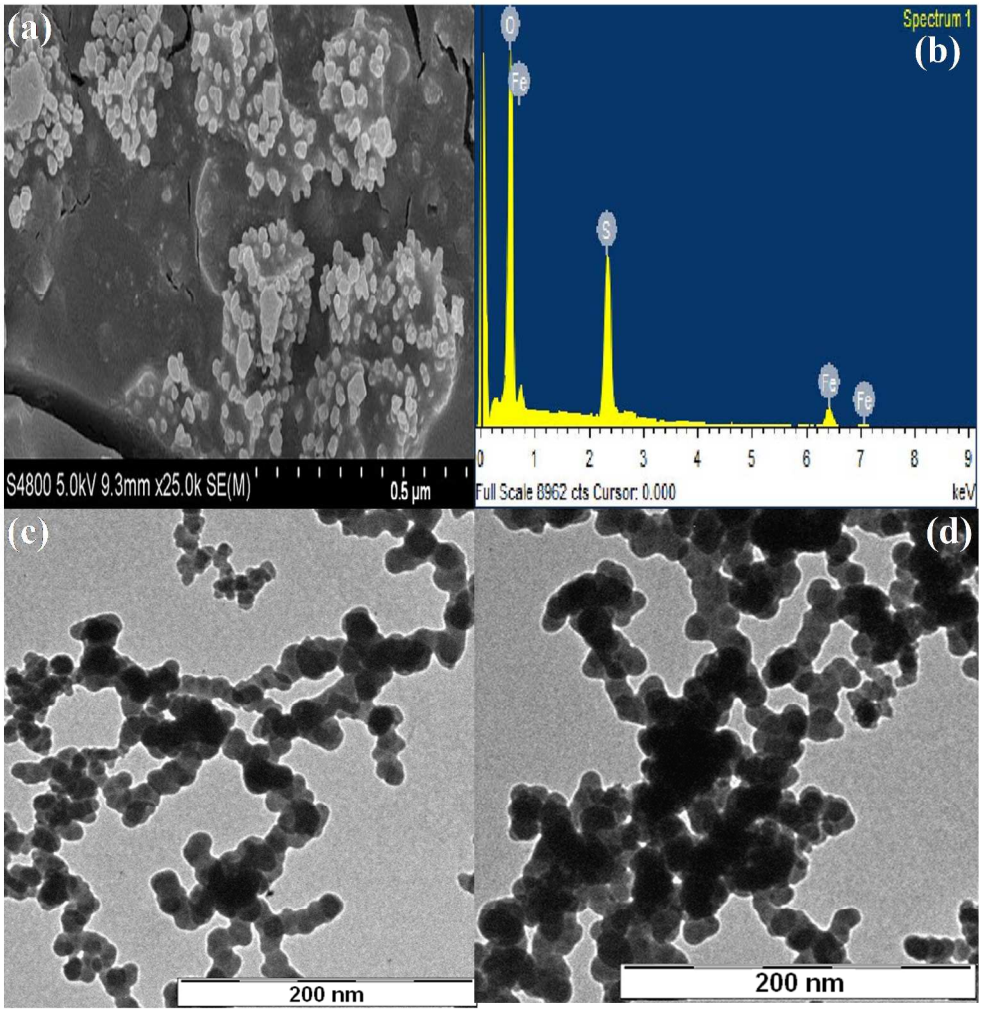

Fig. 7 (a) SEM image of Fe_3O_4-SO_3H NPs; (b) SEM-EDS of Nanocat- Fe_3O_4-SO_3H; and TEM images of Fe_3O_4-SO_3H NPs (c) before use in reaction and (d) after five times applications.

Conclusions

In summary, we have successfully demonstrated a robust and magnetically recoverable Fe_3O_4-SO_3H MNPs catalyzed dehydration reaction for the formation of spirofuran fused eight-membered heterocycles. These potentially bioactivity cyclooctanoid heterocylces have intriguing structural and geometrical features. Most importantly these alkaloids analogous are readily prepared from inexpensive starting materials in moderate to high yield under mild conditions in

air.[17b] In the final step of the synthesis the dehydration reaction for the formation of dihydrofuran ring using Fe_3O_4-SO_3H MNPs was very straightforward, efficient and highly economical. In addition, the employment of iron oxides as acid catalysts is also more environmentally acceptable and safer in terms of toxicity compared to other transition metal catalysts.

Experimental

Solvents and chemicals were purchased from commercial suppliers and used without further purification. Catalyst and starting materials were prepared according to reported procedure. Melting points were measured in open capillary tubes and were uncorrected. Perkin-Elmer 782 spectrophotometer was used for IR spectra. ^1H (300 MHz) and ^{13}C NMR (75 MHz) spectra were performed on Bruker instrument (300 MHz) in DMSO-d_6. Elemental analyses (C, H and N) were recorded using Perkin-Elmer 240C elemental analyzer. The X-ray diffraction data for crystallized compounds were collected with MoKα radiation at 296K using the Bruker APEX-II CCD System. The crystals were positioned at 50 mm from the CCD. Frames were measured with a counting time of 5s. Data analyses were carried out with the Bruker APEX2 and Bruker SAINT program. The structures were solved using direct methods with the Shelxs97 program (Sheldrick, 2008). The morphological analysis of the resultant nanoparticles was confirmed by TEM. The sample suspension is drop casted on a carbon coated copper grid and the excess solution was removed by tissue paper and allowed to air dry at room temperature overnight. TEM study was monitored on a HRTEM, JEOL JEM 2010 at an accelerating voltage of 200kV and fitted with a CCD camera. The crystallinity of synthesized Fe_3O_4 and Fe_3O_4-OSO_3H nanoparticles was determined and confirmed by XRD analysis. The diffractogram was documented from PANalytical, XPERT-PRO diffractrometer using Cu $_\alpha$ (λ= 1.54060) as X-ray

source. Hitachi S-4800 Field Emission Scanning Electron Microscope (Hitachi S-4800 FE-SEM) operating voltage 5.0 kV is used for SEM.

Preparation of Fe_3O_4 nano particle:[19] $FeCl_3 \cdot 6H_2O$ (8.1 g) and urea (5.4 g) were stirred in 300 mL double distilled water at 85 to 90 °C for 2 h. The resultant brown colored reaction mixture was cooled to room temperature and $FeSO_4 \cdot 7H_2O$ (4.2 g) was added into it. The pH of the resultant solution was maintained at 10 by addition of 0.1 M NaOH solution. The molar ratio of Fe(III) to Fe(II) in the above system was nearly 2.0. The obtained hydroxides were kept under ultrasonication in the sealed flask at room temperature for 30 min. After ageing for 5 h, the obtained black powder of Fe_3O_4 nano particles was washed several times with distilled water, and dried under vacuum.

Preparation of Fe_3O_4-SO_3H catalyst:[19] In a two neck round bottom flask, one neck was equipped with a dropping funnel and other neck is fixed with water vacuum to suck HCl gas generated during the reaction. Magnetite, Fe_3O_4 nano particles (3.0 g) was then poured into round bottom flask and neat chlorosulfonic acid was added (1.0 mL) drop by drop over a period of 10 min at room temperature. HCl gas generated immediately from the reaction was removed by suction. After complete addition of chlorosulfonic acid, the mixture was stirred vigorously for 30 min and solid brown magnetic sulfonic acid, Nanocat-Fe-SO_3H (3.45 g) was collected.

Preparation of γ-Fe_3O_4@SiO_2-SO_3H catalyst: [21,22]

Nano-Fe_3O_4@SiO_2 was synthesized according to the previously published literature method.[22] Magnetic Fe_3O_4 nano particles (1.0 g) were initially diluted via the sequential addition of water (20 ml), ethanol (60 ml), and concentrated aqueous ammonia (1.5 ml, 28 wt%). The resulting dispersion was then homogenized by ultrasonic vibration in a water bath. A solution of

TEOS (tetraethyl orthosilicate) (0.45 ml) in ethanol (10 ml) was then added to the dispersion in a drop-wise manner under continuous mechanical stirring. Following a 12 h period of stirring, the resulting γ-Fe_3O_4@SiO_2 nano particles were collected by magnetic separation and washed three times with ethanol.

Chlorosulfonic acid (0.5 g, 4.5 mmol) was added in a drop-wise manner to a cooled (ice-bath) solution of γ-Fe_3O_4@SiO_2 (1.0 g) in *n*-hexane (5 ml) over a period of 2 h. Upon completion of the addition, the mixture was stirred for another 3 h until complete dissipation of HCl occurred from the reaction vessel. The resulting MNPs were separated using an external magnet and washed with methanol before being dried in an oven at 60 °C to give γ-Fe_3O_4@SiO_2-SO_3H as a brown powder.

General synthesis of compounds (±)-**2a-r/2a′-r′**: A mixture of dihydroxy cyclooctanoid heterocylces (±)-**1a-r**/**1a′-r′** (2.0 mmol) and Fe_3O_4-SO_3H (50 mg) in dichloromethane (10.0 mL) was stirred for 10 min (as mentioned in Table 1). When the magnetic stirring of the reaction mixture was discontinued, the magnetic Fe_3O_4-SO_3H MNPs were adsorbed on the surface of the magnetic stirring bar and easily separated from the reaction mixture without filtration. Then dichloromethane was evaporated under vacuum and reaction mass was sonicated with ethylacetate (3 X 10 mL). The combined ethylacetate was evaporated to get yellow solids of (±)-**2a-r**/**2a′-r′**. Yellow solid (±)-**2a-r/2a′-r′** was further purified through crystallization from DMSO solvent.

Spectral Data for Synthesized compounds:

(±)-2a/**2a′**: Yellow amorphous solid, mp: > 300°C, IR (KBr) 3295, 1698 cm^{-1}; ^1H NMR (300 MHz, DMSO-d_6) δ_H 8.67 (t, *J* = 5.7 Hz, 1H), 7.80 (d, *J* = 7.2 Hz, 1H), 7.59 (t, *J* = 6.6 Hz, 1H), 7.44-7.40 (m, 3H), 7.28 (t, *J* = 7.2 Hz, 1H), 7.20 (t, *J* = 6.9 Hz, 1H), 7.07 (d, *J* = 6.9 Hz, 1H),

6.95 (d, *J* = 7.8 Hz, 1H), 6.83-6.77 (m, 2H), 5.41 (s, 1H), 4.15-4.14 (m, 1H), 3.19-3.16 (m, 1H), 2.85-2.81 (m, 2H), 2.12 (s, 3H); ^{13}C NMR (75 MHz, DMSO-d_6) δ_H 191.0, 167.1, 164.4, 155.0, 145.0, 138.7, 134.3, 133.8, 133.7, 131.9, 131.5, 130.8, 130.6, 130.5, 129.3, 124.1, 123.4, 122.8, 120.1, 118.9, 110.0, 102.5, 95.2, 45.0, 40.5, 39.6, 20.8; $C_{27}H_{20}N_2O_3$ (420.47): calcd. C 77.13, H 4.79, N 6.66; found C 77.11, H 4.74, N 6.61.

(±)-2b/**2b′**: Yellow amorphous solid, mp: > 300°C, IR (KBr) 3293, 1701 cm^{-1}; ^{1}H NMR (300 MHz, DMSO-d_6) δ_H 8.82 (t, *J* = 5.4 Hz, 1H), 7.94 (d, *J* = 7.5 Hz, 1H), 7.73-7.68 (m, 1H), 7.57-7.51 (m, 3H), 7.39 (t, *J* = 7.5 Hz, 1H), 7.30 (t, *J* = 7.5 Hz, 1H), 7.17 (d, *J* = 7.2 Hz, 1H), 7.08 (d, *J* = 4.8 Hz, 2H), 5.54 (s, 1H), 4.27-4.25 (m, 1H), 3.33-3.25 (m, 1H), 2.97-2.86 (m, 2H), 2.32 (s, 3H); ^{13}C NMR (75 MHz, DMSO-d_6) δ_H 190.5, 166.7, 164.1, 155.5, 144.2, 138.2, 135.9, 133.9, 133.4, 133.1, 131.2, 130.6, 130.4, 130.2, 126.2, 123.4, 123.2, 122.5, 119.8, 118.6, 112.6, 102.6, 94.1, 44.3, 40.6, 39.6, 20.1; $C_{27}H_{19}ClN_2O_3$ (452.92): calcd. C 71.29, H 4.21, N 6.16; found C 71.41, H 4.14, N 6.10.

(±)-2c/**2c′**: Yellow amorphous solid, mp: > 300°C, IR (KBr) 3286, 1706 cm^{-1}; ^{1}H NMR (300 MHz, DMSO-d_6) δ_H 8.76 (t, *J* = 5.7 Hz, 1H), 7.91 (d, *J* = 7.8 Hz, 1H), 7.63 (t, *J* = 6.9 Hz, 1H), 7.52-7.44 (m, 3H), 7.32 (t, *J* = 7.5 Hz, 1H), 7.23 (t, *J* = 6.9 Hz, 1H), 7.11 (d, *J* = 6.9 Hz, 1H), 7.02-6.99 (m, 2H), 6.89 (d, *J* = 7.8 Hz, 1H), 5.53 (s, 1H), 4.21-4.19 (m, 1H), 3.29-3.24 (m, 1H), 2.91-2.87 (m, 2H); ^{13}C NMR (75 MHz, DMSO-d_6) δ_H 190.5, 166.6, 164.1, 159.6, 156.5, 152.7, 144.2, 138.2, 135.3, 135.2, 133.9, 133.3, 131.1, 130.6, 130.4, 130.2, 123.2, 122.5, 119.8, 118.6, 115.0, 114.7, 110.8, 110.6, 102.7, 94.0, 44.7, 40.6, 39.6; $C_{26}H_{17}FN_2O_3$ (424.44): calcd. C 73.58, H 4.04, N 6.60; found C 73.72, H 3.95, N 6.53.

(±)-2d/**2d′**: Yellow amorphous solid, mp: > 300°C, IR (KBr) 3306, 1699 cm^{-1}; ^{1}H NMR (300 MHz, DMSO-d_6) δ_H 8.86 (br s, 1H), 7.98 (d, *J* = 7.5 Hz, 1H), 7.71 (t, *J* = 6.3 Hz, 1H), 7.59-7.54 (m, 3H), 7.41-7.30 (m, 3H), 7.19-7.06 (m, 3H), 5.59 (s, 1H), 4.32-4.25 (m, 1H), 3.36-3.32 (m, 1H), 2.97-2.93 (m, 2H); ^{13}C NMR (75 MHz, DMSO-d_6) δ_H 190.9, 167.0, 164.5, 155.8, 144.4, 138.6, 136.2, 134.3, 133.8, 131.5, 131.0, 130.7, 130.6, 128.9, 126.5, 123.7, 123.6, 122.9, 120.2, 119.0, 111.9, 103.0, 94.3, 44.8, 40.6, 39.6; $C_{26}H_{17}ClN_2O_3$ (440.89): calcd. C 70.83, H 3.89, N 6.35; found C 70.70, H 3.81, N 6.29.

(±)-2e/**2e′**: Yellow amorphous solid, mp: > 300°C, IR (KBr) 3298, 1704 cm^{-1}; ^{1}H NMR (300 MHz, DMSO-d_6) δ_H 8.79 (t, *J* = 5.7 Hz, 1H), 7.92 (d, *J* = 7.5 Hz, 1H), 7.66 (t, *J* = 6.6 Hz, 1H), 7.53-7.46 (m, 3H), 7.40-7.23 (m, 3H), 7.17-7.12 (m, 2H), 6.99 (d, *J* = 8.7 Hz, 1H), 5.55 (s, 1H), 4.22-4.20 (m, 1H), 3.27-3.26 (m, 1H), 2.92-2.89 (m, 2H); ^{13}C NMR (75 MHz, DMSO-d_6) δ_H 190.9, 167.1, 164.5, 156.3, 144.5, 138.6, 136.7, 134.3, 133.8, 131.8, 131.5, 131.0, 130.8, 130.6, 126.5, 123.6, 122.9, 120.2, 119.0, 114.1, 112.6, 102.9, 94.4, 44.8, 40.6, 39.6; $C_{26}H_{17}BrN_2O_3$ (485.34): calcd. C 64.34, H 3.53, N 5.77; found C 64.49, H 3.47, N 5.70.

(±)-2f/**2f′**: Yellow amorphous solid, mp: > 300°C, IR (KBr) 3301, 1700 cm^{-1}; ^{1}H NMR (300 MHz, DMSO-d_6) δ_H 8.77 (t, *J* = 5.4 Hz, 1H), 7.89 (d, *J* = 7.5 Hz, 1H), 7.67 (t, *J* = 6.9 Hz, 1H), 7.55-7.47 (m, 3H), 7.36 (t, *J* = 7.5 Hz, 1H), 7.27 (t, *J* = 6.9 Hz, 1H), 7.15 (d, *J* = 6.9 Hz, 1H), 6.95 (d, *J* = 8.4 Hz, 1H), 6.78 (d, *J* = 8.4 Hz, 1H), 6.61 (s, 1H), 5.53 (s, 1H), 4.25-4.24 (m, 1H), 3.64 (s, 3H), 3.29-3.27 (m, 1H), 2.95-2.91 (m, 2H); ^{13}C NMR (75 MHz, DMSO-d_6) δ_H 190.6, 166.7, 164.1, 155.3, 150.5, 144.5, 138.3, 134.4, 134.0, 133.2, 131.1, 130.5, 130.4, 130.2, 123.1, 122.4, 119.7, 118.6, 114.1, 110.4, 108.8, 102.4, 94.5, 55.8, 45.1, 40.6, 39.6; $C_{27}H_{20}N_2O_4$ (436.47): calcd. C 74.30, H 4.62, N 6.42; found C 74.42, H 4.56, N 6.47.

(±)-2g/**2g′**: Yellow amorphous solid, mp: > 300°C, IR (KBr) 3299, 1698 cm^{-1}; ^{1}H NMR (300 MHz, DMSO-d_6) δ_H 8.23 (d, J = 6.9 Hz, 1H), 7.91 (d, J = 7.5 Hz, 1H), 7.76-7.69 (m, 2H), 7.60-7.52 (m, 2H), 7.43-7.29 (m, 2H), 7.19 (d, J = 6.9 Hz, 1H), 7.07 (d, J = 7.8 Hz, 1H), 6.95-6.89 (m, 2H), 5.55 (s, 1H), 3.96 (t, J = 13.2 Hz, 1H), 3.37-3.35 (m, 1H), 3.01-2.95 (dd, J_1 = 3.9 Hz, J_2 = 14.1 Hz, 1H), 2.25 (s, 3H), 1.12 (d, J = 11.7 Hz, 3H); ^{13}C NMR (75 MHz, DMSO-d_6) δ_H 190.9, 166.4, 163.3, 154.6, 144.5, 138.4, 133.8, 133.3, 133.0, 131.5, 131.1, 130.5, 130.4, 131.1, 128.9, 123.7, 123.0, 122.5, 119.7, 119.2, 109.5, 102.2, 95.2, 47.5, 45.6, 44.9, 20.4, 17.1; $C_{28}H_{22}N_2O_3$ (434.50): calcd. C 77.40, H 5.10, N 6.45; found C 77.27, H 5.02, N 6.40.

(±)-2h/**2h′**: Yellow amorphous solid, mp: > 300°C, IR (KBr) 3280, 1694 cm^{-1}; ^{1}H NMR (300 MHz, DMSO-d_6) δ_H 8.28 (d, J = 6.3 Hz, 1H), 7.95-7.09 (m, 10H), 5.57 (s, 1H), 3.95 (t, J = 13.5 Hz, 1H), 3.40-3.37 (m, 1H), 3.02-2.98 (dd, J_1 = 2.7 Hz, J_2 = 13.2 Hz, 1H), 2.10 (s, 3H), 1.17 (d, J = 15.6 Hz, 3H); ^{13}C NMR (75 MHz, DMSO-d_6) δ_H 190.8, 166.4, 163.4, 155.5, 144.1, 138.4, 135.8, 133.8, 133.4, 132.6, 131.1, 130.6, 130.3, 130.2, 126.2, 123.3, 123.2, 122.6, 119.8, 119.3, 112.4, 102.6, 94.5, 47.7, 45.5, 44.6, 20.1, 17.1; $C_{28}H_{21}ClN_2O_3$ (468.94): calcd. C 71.72, H 4.51, N 5.97; found C 71.87, H 4.44, N 5.91.

(±)-2i/**2i′**: Yellow amorphous solid, mp: > 300°C, IR (KBr) 3291, 1697 cm^{-1}; ^{1}H NMR (300 MHz, DMSO-d_6) δ_H 8.27 (d, J = 5.7 Hz, 1H), 7.95 (d, J = 5.7 Hz, 1H), 7.73-6.93 (m, 10H), 5.60 (s, 1H), 3.96 (t, J = 13.2 Hz, 1H), 3.35-3.33 (m, 1H), 2.97 (d, J = 12.9 Hz, 1H), 1.15 (d, J = 15.0, 3H); ^{13}C NMR (75 MHz, DMSO-d_6) δ_H 190.7, 166.3, 163.5, 159.6, 156.4, 152.7, 144.0, 138.3, 134.9, 134.8, 133.8, 133.3, 131.1, 130.6, 130.3, 130.2, 123.2, 122.5, 119.8, 119.3, 115.0, 114.7, 110.8, 110.5, 102.8, 94.3, 47.6, 45.5, 45.1, 17.0; $C_{27}H_{19}FN_2O_3$ (438.46): calcd. C 73.96, H 4.37, N 6.39; found C 73.86, H 4.32, N 6.33.

(±)-2j/**2j′**: Yellow amorphous solid, mp: > 300°C, IR (KBr) 3296, 1694 cm^{-1}; ^{1}H NMR (300 MHz, DMSO-d_6) δ_H 8.26 (d, J = 5.7 Hz, 1H), 7.92 (d, J = 7.2 Hz, 1H), 7.73-7.01 (m, 10H), 5.57 (s, 1H), 3.93 (t, J = 12.9 Hz, 1H), 3.37-3.33 (m, 1H), 2.95 (d, J = 11.1 Hz, 1H), 1.12 (d, J = 15.0 Hz, 3H); ^{13}C NMR (75 MHz, DMSO-d_6) δ_H 190.8, 166.4, 163.5, 155.5, 144.0, 138.4, 135.4, 133.8, 133.4, 131.1, 130.7, 130.3, 130.2, 128.5, 126.1, 123.3, 123.2, 122.6, 119.8, 119.3, 111.5, 102.7, 94.3, 47.6, 45.5, 44.7, 17.1; $C_{27}H_{19}ClN_2O_3$ (454.92): calcd. C 71.29, H 4.21, N 6.16; found C 71.18, H 4.16, N 6.10.

(±)-2k/**2k′**: Yellow amorphous solid, mp: > 300°C, IR (KBr) 3299, 1699 cm^{-1}; ^{1}H NMR (300 MHz, DMSO-d_6) δ_H 8.23 (d, J = 6.9 Hz, 1H), 7.91 (d, J = 7.5 Hz, 1H), 7.71-7.65 (m, 2H), 7.52-7.48 (m, 2H), 7.39-7.32 (m, 2H), 7.25 (t, J = 7.2 Hz, 1H), 7.16-7.12 (m, 2H), 6.98 (d, J = 8.4 Hz, 1H), 5.56 (s, 1H), 3.96 (t, J = 13.2 Hz, 1H), 3.30-3.28 (m, 1H), 2.99-2.94 (dd, J_1 = 2.7 Hz, J_2 = 12.9 Hz, 1H), 1.11 (d, J = 15.6 Hz, 3H); ^{13}C NMR (75 MHz, DMSO-d_6) δ_H 191.1, 166.8, 163.8, 156.3, 144.4, 138.7, 136.3, 134.1, 133.8, 131.8, 131.5, 131.1, 130.7, 130.6, 126.4, 123.6, 123.0, 120.2, 119.7, 114.0, 112.5, 103.0, 94.7, 48.0, 45.9, 45.1, 17.4; $C_{27}H_{19}BrN_2O_3$ (499.37): calcd. C 64.94, H 3.84, N 5.61; found C 64.80, H 3.78, N 5.54.

(±)-2l/**2l′**: Yellow amorphous solid, mp: > 300°C, IR (KBr) 3316, 1697 cm^{-1}; ^{1}H NMR (300 MHz, DMSO-d_6) δ_H 8.24 (d, J = 6.6 Hz, 1H), 7.90 (d, J = 7.5 Hz, 1H), 7.75-7.71 (m, 2H), 7.68-7.51 (m, 2H), 7.38 (t, J = 7.2 Hz, 1H), 7.29 (t, J = 6.9 Hz, 1H), 7.17 (d, J = 6.2 Hz, 1H), 6.96 (d, J = 8.7 Hz, 1H), 6.82-6.78 (m, 1H), 6.63 (s, 1H), 5.56 (s, 1H), 3.95 (t, J = 13.5 Hz, 1H), 3.66 (s, 3H), 3.37-3.35 (m, 1H), 3.00-2.95 (dd, J_1 = 3.9 Hz, J_2 = 14.1 Hz, 1H), 1.12 (d, J = 15.6 Hz, 3H); ^{13}C NMR (75 MHz, DMSO-d_6) δ_H 190.9, 166.4, 163.5, 155.2, 150.5, 144.3, 138.4, 133.9, 133.8, 133.3, 133.2, 131.1, 130.4, 130.1, 123.1, 122.5, 119.7, 119.2, 114.1, 110.3, 108.7, 102.4, 94.8,

55.8, 47.6, 45.6, 45.3, 17.1; $C_{28}H_{22}N_2O_4$ (450.50): calcd. C 74.65, H 4.92, N 6.22; found C 74.79, H 4.84, N 6.15.

(±)-2m/**2m′**: Yellow amorphous solid, mp: > 300°C, IR (KBr) 3294, 1692 cm^{-1}; ^1H NMR (300 MHz, DMSO-d_6) δ_H 7.84 (d, *J* = 6.6 Hz, 1H), 7.63 (d, *J* = 7.5 Hz, 1H), 7.51-7.44 (m, 2H), 7.35-7.27 (m, 2H), 7.15 (t, *J* = 7.5 Hz, 1H), 7.07 (t, *J* = 7.2 Hz, 1H), 6.95 (d, *J* = 6.6 Hz, 1H), 6.86 (d, *J* = 7.8 Hz, 1H), 6.68-6.63 (m, 2H), 5.31 (s, 1H), 4.03-4.00 (m, 1H), 2.91-2.88 (m, 1H), 2.01 (s, 3H), 1.53-1.33 (m, 6H), 0.95-0.91 (m, 1H), 0.22-0.18 (m, 1H); ^{13}C NMR (75 MHz, DMSO-d_6) δ_H 190.7, 166.8, 162.4, 154.4, 145.4, 138.3, 134.0, 133.3, 133.2, 131.6, 131.0, 130.3, 130.2, 130.0, 128.7, 123.7, 122.8, 122.4, 119.7, 119.2, 110.0, 104.4, 94.8, 57.2, 53.4, 45.0, 31.0, 30.9, 25.2, 24.3, 20.4; $C_{31}H_{26}N_2O_3$ (474.56): calcd. C 78.46, H 5.52, N 5.90; found C 78.30, H 5.45, N 5.81.

(±)-2n/**2n′**: Yellow amorphous solid, mp: > 300°C, IR (KBr) 3295, 1690 cm^{-1}; ^1H NMR (300 MHz, DMSO-d_6) δ_H 8.13 (d, *J* = 6.9 Hz, 1H), 7.88 (d, *J* = 7.5 Hz, 1H), 7.73-7.65 (m, 2H), 7.58-7.48 (m, 2H), 7.36 (t, *J* = 7.5 Hz, 1H), 7.28 (t, *J* = 7.2 Hz, 1H), 7.15 (d, *J* = 6.9 Hz, 1H), 7.05-7.02 (m, 2H), 5.54 (s, 1H), 4.24-4.01 (m, 1H), 3.12-3.09 (m, 1H), 2.27 (s, 3H), 1.84-1.80 (m, 1H), 1.64-1.55 (m, 5H), 1.17-1.14 (m, 1H), 0.48-0.46 (m, 1H); ^{13}C NMR (75 MHz, DMSO-d_6) δ_H 190.6, 166.9, 162.5, 155.4, 145.1, 138.3, 135.9, 134.1, 133.5, 133.0, 131.1, 130.6, 130.3, 130.0, 126.3, 123.5, 123.0, 122.6, 119.9, 119.4, 112.9, 104.9, 94.3, 57.4, 53.6, 44.8, 31.1, 31.0, 25.3, 24.5, 20.1; $C_{31}H_{25}ClN_2O_3$ (509.01): calcd. C 73.15, H 4.95, N 5.50; found C 73.05, H 4.91, N 5.45.

(±)-2o/**2o′**: Yellow amorphous solid, mp: > 300°C, IR (KBr) 3296, 1687 cm^{-1}; ^1H NMR (300 MHz, DMSO-d_6) δ_H 8.12 (d, *J* = 6.9 Hz, 1H), 7.93 (d, *J* = 6.9 Hz, 1H), 7.75-7.52 (m, 4H), 7.36

(d, *J* = 6.6 Hz, 1H), 7.32 (t, *J* = 6.9 Hz, 1H), 7.19-6.93 (m, 4H), 5.61 (s, 1H), 4.33-4.27 (m, 1H), 3.13-3.07 (m, 1H), 1.87-1.85 (m, 1H), 1.66-1.60 (m, 5H), 1.19-1.15 (m, 1H), 0.48-0.45 (m, 1H); ^{13}C NMR (75 MHz, DMSO-d_6) δ_H 190.5, 166.8, 162.5, 159.7, 156.5, 152.5, 144.9, 138.2, 135.1, 133.9, 133.4, 131.0, 130.2, 129.9, 122.9, 122.4, 119.8, 119.3, 114.8, 114.5, 111.2, 111.1, 110.9, 110.5, 105.0, 94.0, 57.2, 53.5, 45.1, 31.0, 30.9, 25.2, 24.3; $C_{30}H_{23}FN_2O_3$ (478.53): calcd. C 75.30, H 4.84, N 5.85; found C 75.14, H 4.75, N 5.78.

(±)-2p/**2p′**: Yellow amorphous solid, mp: > 300°C, IR (KBr) 3285, 1689 cm^{-1}; ^{1}H NMR (300 MHz, DMSO-d_6) δ_H 8.07 (d, *J* = 6.9 Hz, 1H), 7.88 (d, *J* = 7.8 Hz, 1H), 7.70-7.61 (m, 2H), 7.53-7.46 (m, 2H), 7.32-7.21 (m, 3H), 7.12 (d, *J* = 6.9 Hz, 1H), 7.02-6.97 (m, 2H), 5.55 (s, 1H), 4.31-4.23 (m, 1H), 3.11-3.07 (m, 1H), 1.87-1.84 (m, 1H), 1.61-1.48 (m, 5H), 1.20-1.16 (m, 1H), 0.49-0.45 (m, 1H); ^{13}C NMR (75 MHz, DMSO-d_6) δ_H 190.5, 166.8, 162.5, 155.3, 144.8, 138.2, 135.6, 133.9, 133.4, 131.0, 130.5, 130.2, 129.9, 128.3, 126.2, 123.3, 123.0, 122.5, 119.8, 119.3, 111.9, 104.8, 93.9, 57.2, 53.5, 44.8, 31.0, 30.9, 25.2, 24.4; $C_{30}H_{23}ClN_2O_3$ (494.98): calcd. C 72.80, H 4.68, N 5.66; found C 72.93, H 4.62, N 5.57.

(±)-2q/**2q′**: Yellow amorphous solid, mp: > 300°C, IR (KBr) 3299, 1685 cm^{-1}; ^{1}H NMR (300 MHz, DMSO-d_6) δ_H 8.14 (d, *J* = 6.9 Hz, 1H), 7.94 (d, *J* = 7.5 Hz, 1H), 7.76-7.68 (m, 2H), 7.59-7.46 (m, 3H), 7.39 (t, *J* = 7.5 Hz, 1H), 7.31 (t, *J* = 7.5 Hz, 1H), 7.21-7.17 (m, 2H), 7.02 (d, *J* = 8.4 Hz, 1H), 5.62 (s, 1H), 4.31-4.23 (m, 1H), 3.11-3.07 (m, 1H), 1.87-1.84 (m, 1H), 1.67-1.54 (m, 5H), 1.20-1.16 (m, 1H), 0.49-0.45 (m, 1H); ^{13}C NMR (75 MHz, DMSO-d_6) δ_H 190.9, 167.2, 162.8, 156.1, 145.2, 138.6, 136.4, 134.3, 133.8, 131.6, 131.4, 130.9, 130.6, 130.2, 126.4, 123.4, 122.9, 120.2, 119.7, 114.1, 112.9, 105.1, 94.3, 57.6, 53.9, 45.1, 31.4, 31.3, 25.5, 24.7; $C_{30}H_{23}BrN_2O_3$ (539.43): calcd. C 66.80, H 4.30, N 5.19; found C 66.95, H 4.26, N 5.12.

(±)-2r/2r′: Yellow amorphous solid, mp: > 300°C, IR (KBr) 3290, 1692 cm^{-1}; ^{1}H NMR (300 MHz, DMSO-d_6) δ_H 8.09 (d, J = 7.2 Hz, 1H), 7.88 (d, J = 7.5 Hz, 1H), 7.75-7.67 (m, 2H), 7.58-7.50 (m, 2H), 7.41 (t, J = 6.6 Hz, 1H), 7.33 (t, J = 10.8 Hz, 1H), 7.18 (d, J = 6.9 Hz, 1H), 6.95 (d, J = 8.7 Hz, 1H), 6.85 (dd, J_1 = 1.8 Hz, J_2 = 8.7 Hz, 1H), 6.62 (s, 1H), 5.57 (s, 1H), 4.28-4.26 (m, 1H), 3.68 (m, 3H), 3.16-3.12 (m, 1H), 1.83-1.80 (m, 1H), 1.69-1.58 (m, 5H), 1.21-1.20 (m, 1H), 0.48-0.47 (m, 1H); ^{13}C NMR (75 MHz, DMSO-d_6) δ_H 191.0, 167.2, 162.8, 155.8, 150.7, 145.6, 138.7, 134.5, 134.4, 133.6, 131.3, 130.7, 130.5, 130.4, 123.2, 122.8, 120.1, 119.6, 114.2, 111.1, 109.3, 105.0, 94.9, 57.6, 56.3, 53.8, 45.8, 31.4, 31.2, 25.6, 24.7; $C_{31}H_{26}N_2O_4$ (490.56): calcd. C 75.90, H 5.34, N 5.71; found C 75.78, H 5.30, N 5.66.

Acknowledgements

S.P. and K.D. thank CSIR and UGC, New Delhi, India, for offering them Senior Research Fellowship (SRF) respectively. The author Md. M. R. Mollick gratefully acknowledge the Department of Science & Technology (DST), Govt. of India for providing fellowship under the INSPIRE program. The financial assistance of CSIR, New Delhi is gratefully acknowledged [Major Research Project, No. 02(0007)/11/EMR-II]. Crystallography was performed at the DST-FIST, India-funded Single Crystal Diffractometer Facility at the Department of Chemistry, University of Calcutta. We also acknowledge Center for Research in Nanoscience and Nanotechnology (CRNN), University of Calcutta for instrumental facilities.

References:

1 G. Mehta and V. Singh, *Chem. Rev.*, 1999**, 99**, 881–930.

2 N. A. Petasis and M. A. Patane, *Tetrahedron*, 1992, **48**, 5757–5821.

3 (a) S. Huneck, G. Baxter, A. F. Cameron, J. D. Connelly and D. S. Rycroft, *Tetrahedron Lett.*, 1983, **24**, 3787-3788; (b) J. Zapp, G. Burkhardt and H. Becker, *Phytochemistry*, 1994, **37**, 787-793; (c) H.-J. Liu, C.-L. Wu, H. Becker and J. Zapp, *Phytochemistry*, 2000, **53**, 845-849; (d) F. Huang, Z. -K Yao, Y. Wang, Y. Wang, J. Zhang and Z. –X. Yu, *Chem. Asian J.*, 2010, **5**, 1555–1559.

4 (a) L. Erguang, A. M. Clark, D. P. Rotella and C. D. Hufford, *J. Nat. Prod.*, 1995, **58**, 74-81.

5 W. H. Pearson, I. Y. Lee, Y. Mi and P. Stoy, *J. Org. Chem.*, 2004, **69**, 9109-9122.

6 K. Tsuna, N. Noguchi and M. Nakada, *Angew. Chem. Int. Ed.*, 2011, **50**, 9452-9455.

7 H. Qin, Z. Xu, Y. Cui and Y. Jia, *Angew. Chem. Int. Ed.*, 2011, **50**, 4447-4449.

8 T. H. Quang, D. –S. Lee, J. H. Sohn, Y. –C. Kim and H. Oh, *Bull. Korean Chem. Soc.*, 2013, **34**, 3109-3112.

9 H. Zhang, S. Qiu, P. Tamez, G. T. Tan, Z. Aydogmus, N. Van Hung, N. M. Cuong, C. Angerhofer, D. D. Soejarto, J. M. Pezzuto and H. H. S. Fong, *Pharm. Biol.*, 2002, **40**, 221-224.

10 T. –S. Kam, K. Yoganathan, T. Koyano and K. Komiyama, *Tetrahedron Lett.,* 1996, **37**, 5765-5768.

11 (a) L. Mitchell, J. A. Parkinson, J. M. Percy and K. Singh, *J. Org. Chem.*, 2008, **73**, 2389-2395; (b) C. J. Creighton and A. B. Reitz, *Org. lett.*, 2001, **3**, 893-895; (c) N. Brown, B. Xie, N. Markina, D. VanderVelde, J. –P. H. Perchellet, E. M. Perchellet, K R. Crow and K. R. Buszek, *Bioorg. Med. Chem. Lett.*, 2008, **18**, 4876-4879; (d) S. K. Chattopadhyay, S. Karmakar, T. Biswas, K. C. Majumdar, H. Rahaman and B. Roy, *Tetrahedron*, 2007, **63**, 3919-3952; (e) K. C. Majumdar, S. Samanta, B. Chattopadhyay and R. K. Nandi, *Synthesis*, 2010, 863-869.

12 C. J. Roxburgh, *Tetrahedron*, 1993**, 49***,* 10749–10784.

13 F. Genrich and E. Schaumann, *Tetrahedron Lett.*, 2009, **50**, 6187–6190.

14 S. L. G. Ayala, E. Stashenko, A. Palma, A. Bahsas and J. M. Amaro-Luis, *Synlett*, 2006, **14**, 2275-2277.

15 T. Zhang, X. Huang, J. Xue and S. Sun, *Tetrahedron Lett.*, 2009, **50**, 1290–1294.

16 (a) M. Mascal, K. V. Modes and A. Durmus, *Angew. Chem. Int. Ed.*, 2011, **50**, 4445-4446; (b) A. Sharma, P. Appukkuttan and E. Van der Eycken, *Chem. Commun.*, 2012, **48**, 1623-1637; (c) K. Wittstein, K. Kumar and H. Waldmann, *Angew. Chem. Int. Ed*., 2011, **50**, 9076-9080; (d) M. M. Coulter, P. K. Dornan and V. M. Dong, *J. Am. Chem. Soc.*, 2009, **131**, 6932-6933; (e) H. Qin, Z. Xu, Y. Cui and Y. Jia, *Angew. Chem. Int. Ed*., 2011, **50**, 4447-4449; (f) A. Mishra and S. Batra, *Eur. J. Org. Chem.*, 2010, 4832–4840; (g) P. G. Jones, *Organometallics*, 2012, **31**, 3361-3372; (h) R. Pflantz, J. Sluiter, M. Krička, W. Saak, C. Hoenke and J. Christoffers, *Eur. J. Org. Chem.*, 2009, 5431–5436; (i) S. López-Tosco, D. Tejedor, J. González-Platas and F. García-Tellado, *Eur. J. Org. Chem.*, 2011, 6847–6850; (j) V. A. Peshkov, S. Van Hove, P. A. Donets, O. P. Pereshivko, K. Van Hecke, L. Van Meervelt and E. V. Van der Eycken, *Eur. J. Org. Chem.*, 2011, 1837–1840.

17 (a) S. Das, R. Fröhlich and A. Pramanik, *Org. Lett*., 2006, **8**, 4263-4266; (b) S. Pathak and A. Pramanik, *Eur. J. Org. Chem.*, 2013, 4410–4417; (c) S. Das, P. Koley and A. Pramanik, *Tetrahedron Lett*., 2011, **52**, 3243-3246; (d) S. Pathak, A. Kundu and A. Pramanik, *Tetrahedron Lett.*, 2011, **52**, 5180-5183; (e) S. Pathak, K. Debnath and A. Pramanik, *Beilstein J. Org. Chem.*, 2013, **9**, 2344–2353; (f) S. Das, A. Pramanik, R. Fröhlich and A. Patra, *Tetrahedron*, 2004, **60**, 10197-10205; (g) S. Pathak, K. Debnath, Sk T. Hossain, S. K. Mukherjee and A. Pramanik, *Tetrahedron Lett*., 2013, **54**, 3137–3143; (h) K. Debnath, S. Pathak and A. Pramanik, *Tetrahedron Lett*., 2013, **54**, 4110–4115; (i) K. Debnath, S. Pathak and A. Pramanik, *Tetrahedron Lett*., 2014, **55**, 1743–1748.

18 (a) V. Polshettiwar, R. Luque, A. Fihri, H. Zhu, M. Bouhrara and J. –M. Basset, *Chem. Rev.* 2011, **111**, 3036–3075; (b) R. B. N. Baig and R. S. Varma, *Chem. Commun.*, 2013, **49**, 752-770; (c) S. Shylesh, V. V. Schünemann and W. R. Thiel, *Angew. Chem. Int. Ed.*, 2010, **49**, 3428–3459; (d) M. Shafiee, A. R. Khosropour, I. Mohammadpoor-Baltork, M. Moghadam, S. Tangestaninejad and V. Mirkhani, *Catal. Sci. Technol.,* 2012, **2**, 2440–2444; (e) A. Wang, X. Liu, Z. Su and H. Jing, *Catal. Sci. Technol.*, 2014, **4**, 71–80.

19 (a) C. G. Piscopo, S. Bühler, G. Sartori and R. Maggi, *Catal. Sci. Technol.*, 2012, **2**, 2449–2452; (b) M. B. Gawande, A. K. Rathi, I. D. Nogueira, R. S. Varma and P. S. Branco, *Green Chem.*, 2013, **15**, 1895.

20 E. Kolvari, N. Koukabi and O. Armandpour, *Tetrahedron*, 2014, **70**, 1383-1386.

21. F. Nemati, M. M. Heravi and R. S. Rad, *Chinese J. Catal.*, 2012, **33**, 1825–1831.

22. D. Yang, J. Hu and S. Fu, *J Phys Chem C*, 2009, **113**, 7646-7651.